NMR Constraints on the Location of the Retinal Chromophore in Rhodopsin and Bathorhodopsin†

May Han and Steven O. Smith*

Department of Molecular Biophysics and Biochemistry, Yale University, 266 Whitney Avenue, P.O. Box 208114, New Haven, Connecticut 06520-8114

Received September 29, 1994; Revised Manuscript Received November 17, 1994®

ABSTRACT: Rhodopsin is the photoreceptor in vertebrate rod cells responsible for vision at low light intensities. The photoreactive chromophore in rhodopsin is 11-*cis*-retinal bound to the protein via a protonated Schiff base with Glu113 as the counterion. We have used the observed ^{13}C NMR chemical shifts of the conjugated retinal carbons in combination with semiempirical molecular orbital calculations to establish the major charge interactions in the retinal binding site of rhodopsin and its primary photoproduct, bathorhodopsin. In rhodopsin, the NMR data constrain one of the carboxylate oxygens (O_1) of Glu113 to be ~3 Å from the C_{12} position of the retinal with the second oxygen oriented away from the conjugated retinal chain. The $O_1-C_{12}-H$ angle is constrained by taking into account the 500 nm absorption maximum of the protein-bound retinal as well as the chemical shift data. The bathorhodopsin retinal binding site structure is generated from the rhodopsin model by isomerization of the $C_{11}=C_{12}$ bond and incorporation of C−C single bond twists from C_8 to C_{15}. The resulting structure yields a moderate fit to both the chemical shift data and the 543 nm absorption maximum of bathorhodopsin. In both the rhodopsin and bathorhodopsin models, we have included a structural water molecule hydrogen bonded with the Schiff base to account for the high C=N stretching vibrations previously observed. Finally, the retinal binding site structure derived from the NMR constraints is used to position the 11-*cis*-retinal chromophore in the interior of a structural model of the rhodopsin apoprotein recently proposed on the basis of sequence analysis of G-protein-coupled receptors [Baldwin, J. (1993) *EMBO J. 12,* 1693−1703].

The visual pigment rhodopsin belongs to a large and growing family of G-protein-coupled receptors having seven transmembrane helices (Oprian, 1992; Strader et al., 1994). 11-*cis*-Retinal (Figure 1) is the photoreactive group in rhodopsin and is bound in the interior of the protein through a covalent protonated Schiff base (PSB)[1] linkage to Lys296. The photochemistry of the retinal chromophore and its interactions with surrounding protein residues have been intensively studied in an effort to understand how absorbed light energy is converted into a chemical signal. Mutagenesis studies from several groups have shown that the negatively charged counterion to the PSB is the carboxylate side chain of Glu113 (Nathans, 1990; Zhukovsky & Oprian, 1989; Sakmar et al., 1989). The electrostatic interaction between the retinal PSB and Glu113 contributes to locking the protein in an inactive state in the dark (Cohen et al., 1992; Robinson et al., 1992) and also serves to red-shift the absorption spectrum of the chromophore to the visible region (Nathans, 1990; Zhukovsky & Oprian, 1989; Sakmar et al., 1989). Protein activation results from light-driven 11-*cis* → *trans* isomerization of the retinal and deprotonation of the Schiff base nitrogen. The Schiff base proton may be transferred to Glu113 which has been shown to protonate in the formation of metarhodopsin II (Fahmy et al., 1993; Jäger et al., 1994), the intermediate that interacts with and activates the G-protein transducin (Kühn, 1980). Neutralization of Glu113, rather than the deprotonation of the PSB *per se*, seems to be essential for rhodopsin activation (Zvyaga et al., 1994). The key to understanding the reaction mechanism

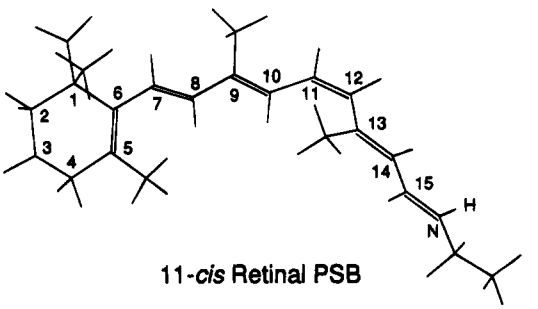

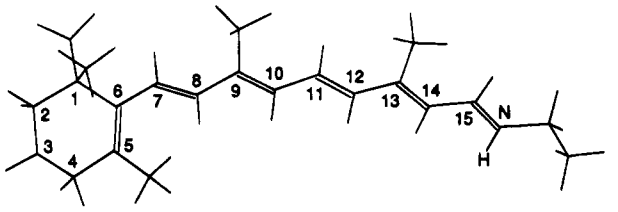

FIGURE 1: Structures of the 11-*cis*- and *all-trans*-retinylidene PSB chromophores.

† This work was supported by the National Institutes of Health (GM-41412).

® Abstract published in *Advance ACS Abstracts,* January 1, 1995.

[1] Abbreviations: MNDO, modified neglect of differential overlap; PSB, protonated Schiff base; NMR, nuclear magnetic resonance; ZDO, zero differential overlap; HOOP, hydrogen-out-of-plane.

0006-2960/95/0434-1425$09.00/0

of rhodopsin lies in determining the structure of the retinal binding site and in defining the charge interactions between the retinal PSB and Glu113 in both rhodopsin and its photointermediates.

The retinal chromophore in rhodopsin is a conjugated polyene whose electronic structure is extremely sensitive to surrounding protein charges. This sensitivity can be mainly attributed to protonation of the retinal−lysine Schiff base linkage which adds a net positive charge to the molecule. For retinal PSB model compounds in hydrophobic solvents, partial positive charge becomes localized on the Schiff base proton and adjacent odd numbered carbons, C_{15} and C_{13}, as a result of close association of the negative counterion. In the protein binding sites of rhodopsin, charge delocalization leading to spectral red-shifts may result from simply increasing the separation between the PSB and its associated counterion (Blatz et al., 1972) or from placing charged or polar residues along the conjugated chain that stabilize partial positive charge on the retinal carbons away from the PSB (Honig et al., 1976; Kropf & Hubbard, 1958). Over the past 20 years, a number of models have been proposed for the structure of the retinal binding site in rhodopsin and the location of charged residues interacting with the retinal. On the basis of absorption spectra of rhodopsin regenerated with a series of dihydroretinals, Honig et al. (1979) argued that the chromophore interacts with two negative charges in its protein binding site. One charge acts as a counterion to the PSB, while a second charge situated near the middle of the retinal chain generates a red-shift in the chromophore's absorption band. A more recent data set obtained of dihydroretinal pigments in native membranes has led to a model where the second charge is situated near C_{13} (Koutalos et al., 1989). Birge and co-workers have shown that the binding site is neutral (Birge et al., 1985) and have argued that the counterion is not directly associated with the Schiff base (Birge et al., 1988). They have proposed a model based on low temperature actinometry, absorption spectroscopy, and semiempirical molecular orbital calculations where the two carboxylate oxygens bearing partial negative charges interact with positions C_{13} and C_{15} of the retinal (Birge et al., 1988; Tallent et al., 1992). These studies provide rough constraints on the position of the counterion.

We have studied the structure of the retinal binding site of both rhodopsin and its photointermediates using ^{13}C magic angle spinning NMR (Smith et al., 1990, 1991). The ^{13}C NMR chemical shift is sensitive to the electron density surrounding the carbon nucleus and provides a probe of the partial charge on *each* carbon of the conjugated retinal chain. The advantage of NMR over vibrational and absorption measurements is that the observed chemical shifts reflect the local charge density at each conjugated carbon as well as provide global information when the electron density *profile* along the conjugated retinal chain is considered. In addition, the chemical shift data are obtained on the native protein sparing the complications in data interpretation that sometimes are encountered using retinal analogs or rhodopsin mutants. We have been able to roughly establish the position of the Glu113 counterion relative to the retinal PSB in rhodopsin using the constraints derived from the chemical shifts of the conjugated carbons (Han et al., 1993).

In this paper, we further refine the geometry of the retinal binding site in rhodopsin by combining constraints imposed by the NMR chemical shift and the visible absorption data. We also propose a model for the principal charge interactions in bathorhodopsin. Bathorhodopsin is formed from rhodopsin by a rapid photochemical isomerization of the C_{11}=C_{12} bond and is ~33 kcal/mol higher in energy than the parent rhodopsin pigment (Schick et al., 1987; Cooper, 1979). The energy stored in bathorhodopsin is used to drive the subsequent thermal reactions of the pigment, leading to protein conformational changes at the metarhodopsin II intermediate which trigger G-protein activation (Resek 1993; Rothschild et al., 1987). Finally, on the basis of the rhodopsin binding site model, we are able to position the retinal chromophore in a recent structural model of the rhodopsin apoprotein (Baldwin, 1993).

MATERIALS AND METHODS

The retinal ^{13}C chemical shifts for rhodopsin and bathorhodopsin were previously obtained using magic angle spinning NMR (Smith et al., 1990, 1991). The charge densities on the retinal for different binding site structures are obtained from semiempirical calculations with the program ZINDO using the ZDO basis set (Zerner, Florida State University). For each conjugated carbon, the charge density can be related to the chemical shift by using a linear correlation of 160 ppm per unit charge (Spiesecke & Schneider, 1961; Lauterbur, 1961; Tokuhiro & Fraenkel, 1969). The best correlations between calculated charge densities and the experimental chemical shift data are found when the *differences* rather than the absolute values are considered between two closely related compounds (Rodman-Gilson & Honig, 1988). In this study, 11-*cis*-*N*-retinylidene-*n*-propyliminium chloride (11-*cis*-RPSB$\cdot Cl^-$) and *all-trans*-*N*-retinylidene-*n*-propyliminium chloride (*all-trans*-RPSB$\cdot Cl^-$) model compounds in CCl_3D (Shriver et al., 1976, 1979) are used as the reference states for rhodopsin and bathorhodopsin, respectively. The calculated charge density difference on each conjugated carbon between a given structural model and the reference can be converted to a chemical shift difference through the 160 ppm/unit charge correlation. A qualitative comparison can be made by overlaying the profiles of the calculated and experimental chemical shift differences for the conjugated carbons along the chain. A quantitative evaluation is made by plotting the experimental chemical shift differences against the calculated charge density differences and determining the linear correlation of the data points. The geometry of the 11-*cis*-retinal PSB used in this study was derived from the crystal structure of 11-*cis*-retinal (Gilardi et al., 1972) and was energy minimized using the MOPAC program (Dewar, University of Texas) with the MNDO Hamiltonian while holding the C_5−C_6−C_7−C_8 and C_{11}−C_{12}−C_{13}−C_{14} torsion angles at 45° and −140°, respectively (Honig & Karplus, 1971; Gilardi et al., 1972; Birge et al., 1988). The geometry of the *all-trans*-RPSB$\cdot Cl^-$ was obtained by isomerizing the C_{11}=C_{12} bond of the 11-*cis*-RPSB$\cdot Cl^-$, removing the C_{12}−C_{13} twist, and energy minimizing the structure while holding the C_5−C_6−C_7−C_8 torsion angle at 45°. The structure of the two retinal PSBs are shown in Figure 1. The absorption maxima are derived from the $S_0 \rightarrow S_1$ transition energies obtained using the ZINDO program taking into account both single and double configuration interactions. Calculations for several model compounds were first carried out to test the

Table 1: Comparison of the Calculated and Experimental Absorption Maxima for *all-trans*-Retinal Model Compounds, Rhodopsin, and Bathorhodopsin

compound	λ_{max} (experimental) (nm)	λ_{max} (calculated) (nm)
all-trans-RPSB·Cl	442[a]	447
all-trans-RPSB·Br	451[a]	457
rhodopsin	500	503
bathorhodopsin	543	534

[a] Data from Blatz et al. (1972) taken in CCl_4.

accuracy of the method. Table 1 summarizes the calculated and experimental λ_{max} for *all-trans* model compounds as well as for rhodopsin and bathorhodopsin.

RESULTS AND DISCUSSION

Over the past two decades, considerable effort has been directed at establishing the structure of the retinal binding site in rhodopsin and the structural changes that occur upon photoreaction of the 11-*cis*-retinal chromophore. These studies address the general question of how retinal isomerization is coupled to G-protein activation. Specific questions underlying this research include how the protein red-shifts the visible absorption spectrum of the chromophore and how photochemical energy is stored in the bathorhodopsin intermediate and channeled into the protein. In the first two sections below, we describe the constraints imposed by the NMR chemical shift data on the structure of the retinal binding sites in rhodopsin and bathorhodopsin. In the last section, we use the NMR constraints along with biochemical data to position the retinal chromophore in a structural model of rhodopsin apoprotein recently developed by Baldwin (1993).

Location of Glu113 in the Retinal Binding Site of Rhodopsin. The position of the Glu113 counterion was previously localized by analyzing the ^{13}C chemical shifts of the conjugated retinal carbons (Han et al., 1993). There are two unusual features of the experimental chemical shift or charge density differences for the protein-bound retinal when compared to the 11-*cis* PSB reference state. First, the chemical shifts are *uniformly* shifted upfield from C_6 to C_{14}, in contrast to an *alternating* pattern of chemical shift differences generally observed when retinal model compounds are compared (Han et al., 1993). Second, large shifts are observed at the normally insensitive even-numbered positions C_{10} and C_{12} (Albeck et al., 1992). We found that the pattern of chemical shift differences from C_5 to C_{14} could only be fit by placing one of the oxygens (O_1) of the carboxylate counterion ~3.0 Å from C_{12}. The second oxygen (O_2) must be oriented away from the conjugated chain. The position of the charge relative to the retinal plane, however, was relatively unconstrained (Han et al., 1993). In this study, we were able to refine the position of the carboxylate counterion by considering the calculated absorption maximum of the pigment as a function of the O_1–C_{12}–H_{12} angle θ.

A series of calculations of charge densities and λ_{max} were carried out where the angle θ was changed from −120° to 120° in increments of 15°. The O_1–C_{12} distance was maintained at 3.0 Å, and the O_1–H_{12}–C_{12} plane was kept perpendicular to the retinal plane. Since the 11-*cis* PSB chromophore is not strictly planar due to the twists of the C_6–C_7 and C_{12}–C_{13} single bonds, we refer to the "retinal plane" as the planar segment from C_7 to C_{13}. We define a linear O_1–H_{12}–C_{12} geometry, where O_1 is in the plane of the retinal, as 0° and a linear H_{12}–C_{12}–O_1 geometry as 180°. The angle θ is defined as positive when O_1 is on the opposite side of the retinal plane from the C_{13} methyl group. The ±120° limits are chosen to avoid van der Waals contact between the charge and the C_{13} methyl. The second oxygen of the carboxylate group (O_2) is maintained at a maximal distance from C_{12}.

Figure 2a presents the calculated absorption maxima as a function of the angle θ. Orientations between −15° and 60° yield calculated λ_{max} values within ±10 nm of the 500 nm absorption maximum of rhodopsin. The chemical shift data restrict the angle to be between −45° and 90°; this agrees with the earlier study using a simple point charge counterion (Han et al., 1993). Positioning the carboxylate group at 60° (Figure 2d) yields a λ_{max} of 503 nm as well as good agreement between the calculated and observed charge density differences with a correlation factor of 0.91 (Figure 2b,c). The most out-of-plane orientation ($\theta = 60°$) is chosen as our working model for reasons discussed below in connection with bathorhodopsin, although other geometries shown to be acceptable by both NMR and λ_{max} constraints are by no means ruled out.

Figure 2b clearly shows that the unusual pattern of chemical shift differences between rhodopsin and the reference compound are reproduced by the model. Placing the counterion closest to C_{12} results in an increase of partial positive charge on the odd-numbered conjugated carbons and a decrease of partial negative charge on the even-numbered carbons. Both effects yield upfield chemical shifts. The total electron density repulsed from the retinal chain is calculated to be 0.112 e^- from C_5 to C_{15}. Electron density migrates mainly to the Schiff base. The electronegative Schiff base nitrogen gains 0.059 e^- and the Schiff base proton gains 0.038 e^-. The remaining negative charge is dispersed among the nonconjugated retinal atoms.

The model in Figure 2d incorporates a water molecule hydrogen bonded to the Schiff base to account for the high C=N stretching frequency (~1660 cm^{-1}) and large ND isotope shift (~30 cm^{-1}) which indicate that the SB is strongly hydrogen-bonded (Mathies et al., 1977; Narva & Callender, 1980; Bagley et al., 1985; Rodman-Gilson et al., 1988; Bassov et al., 1987), possibly due to water in the binding site (Rafferty & Shichi, 1981; Cossette & Vocelle, 1987; Tallent et al., 1992). New evidence for water bound near the SB in rhodopsin comes from the recent observation of rapid hydrogen/deuterium exchange of the Schiff base proton (Deng et al., 1994). It is important to consider the implications of water in the binding site in the context of the function of rhodopsin. Structural water is thought to be important for maintaining the unusually high pK_a of the Schiff base in rhodopsin which is estimated to be greater than 16 (Steinberg et al., 1993; Birge, 1993). Gat and Sheves (1993) have shown, on the basis of an elegant set of retinal model compounds, that the pK_a can be increased by specific orientations of the Schiff base and carboxylate counterion which allow structural water molecules to bridge these groups. The high pK_a of the Schiff base is critical since maintaining the salt bridge between Glu113 and the retinal PSB contributes to locking the protein in an inactive state (Cohen et al., 1992; Robinson et al., 1992). A stable protonated Schiff base also keeps the protein absorbing in the visible range. Schiff base deprotonation may simply

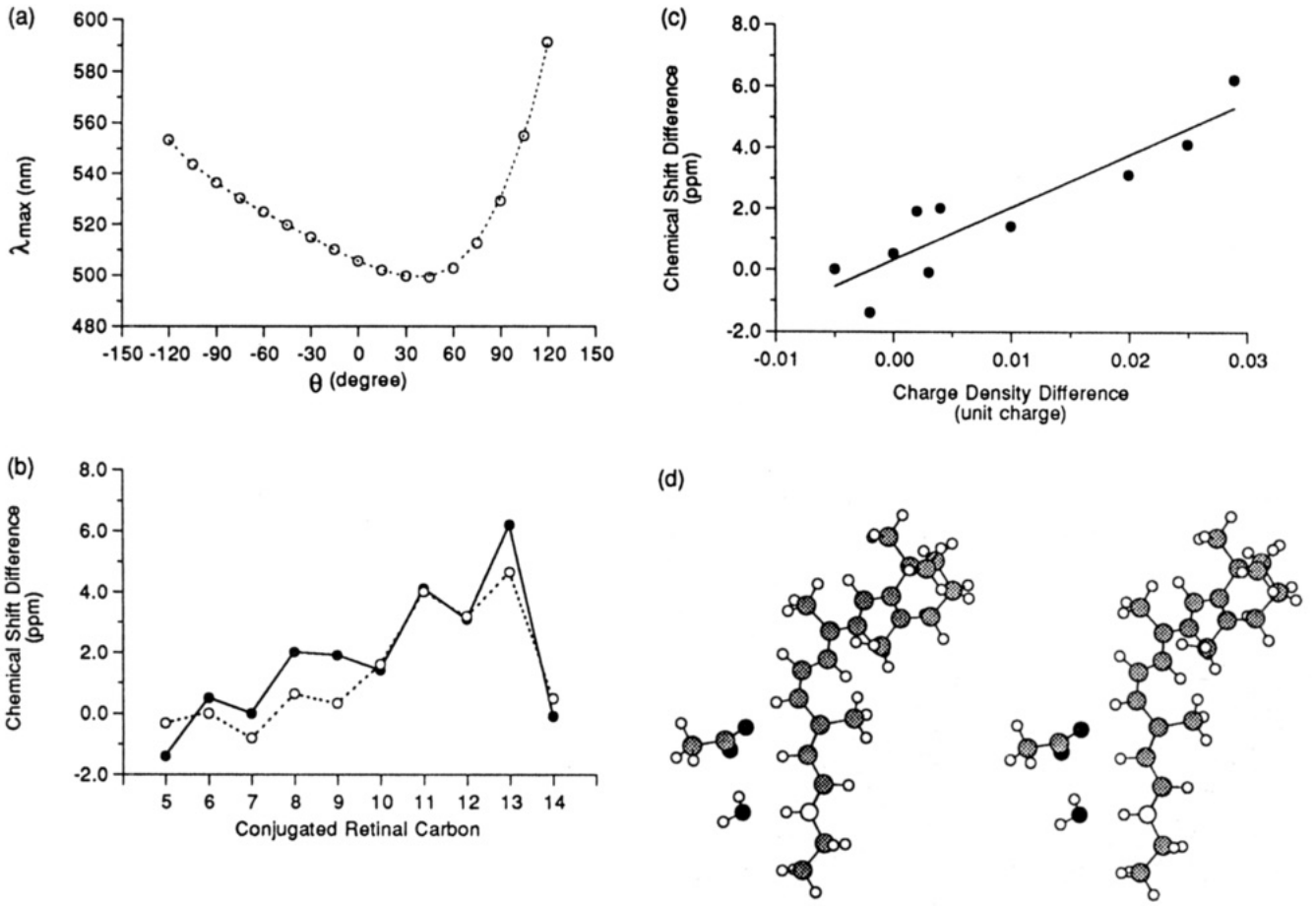

FIGURE 2: Modeling the retinal binding site of rhodopsin. (a) Calculated absorption maxima as a function of the O_1╍C_{12}╍H angle θ from $-120°$ to 120° in an increments of 15° (○). The calculated data points are fit with a smooth curve (dotted line). (b) Comparison of experimental (●) and calculated (○) chemical shift differences for rhodopsin and the model shown in (panel d). 11-*cis*-RPSB-Cl is used as the reference state. (c) Linear correlation of the chemical shift data with the calculated charge densities of the model. The correlation coefficient of 0.91, the slope of 172 ppm/unit charge, and the intercept of 0.29 ppm represent good fits. (d) Retinal binding site model with a CH_3-COO^- counterion and H_2O hydrogen bonded at the Schiff base. Black symbols stand for O, gray for C, white for N, and small white symbols for H. The key distances are O_1╍C_{12} (CH_3-COO^-) 3.0 Å, O_1╍H_{12} 2.6 Å, O_1╍C_{11} 3.5 Å, O_1╍C_{13} 3.6 Å, O_1╍N 4.7 Å, O_2╍C_{12} (CH_3-COO^-) 5.1 Å, and N╍O (water) 2.9 Å.

result from changes in the orientation of the Schiff base relative to the counterion due to retinal isomerization (Gat & Sheves, 1993; Scheiner & Duan, 1991; Scheiner & Hillenbrand, 1985). In our current model, as well as the one previously proposed, the H_2O is oriented such that its oxygen forms an optimal hydrogen bond with the N−H proton and one of the O−H protons forms a weaker hydrogen bond with the O_2 oxygen of the carboxylate counterion. It is possible that two or more H_2O molecules are present in the binding site and are involved in a more extensive hydrogen bonding network.

Location of Glu113 in the Retinal Binding Site of Bathorhodopsin. Absorption of light by rhodopsin leads to rapid isomerization of the retinal chromophore. Transient absorption measurements indicate that bathorhodopsin forms in ~40 ps (Schoenlein et al., 1991). The retinal in bathorhodopsin is conformationally distorted based on the observation of intense hydrogen out-of-plane (HOOP) modes in the resonance Raman spectrum (Eyring et al., 1982; Palings et al., 1989). Interestingly, the coupled $C_{11}H$═$C_{12}H$ HOOP observed in rhodopsin and retinal model compounds is *uncoupled* in bathorhodopsin (Eyring et al., 1982; Palings et al., 1989), possibly due to a change in the Glu113╍retinal interaction. Calorimetry measurements have indicated that bathorhodopsin stores ~33 kcal/mol of the absorbed light energy (Schick et al., 1987; Cooper, 1979). On the basis of low temperature absorption measurements and quantum chemical calculations, Birge and co-workers (Birge et al., 1988) estimated that energy storage in bathorhodopsin could be partitioned into conformational distortions of the protein and retinal (60%) and charge separation between the retinal PSB and the protein counterion (40%).

We have previously measured the NMR chemical shifts in bathorhodopsin at positions C_{10} through C_{15} and C_8 (Smith et al., 1991). The experimental chemical shift differences between bathorhodopsin and the *all-trans* RPSB reference (Figure 3a, filled circles) are strikingly similar to those observed for rhodopsin (Figure 2b, filled circles). Upfield shifts are observed for the conjugated carbons in the middle of the retinal chain from C_{10} to C_{14}, including the normally insensitive even-numbered positions C_{10} and C_{12}. As in rhodopsin, the large upfield shift at C_{12} cannot be explained by C−C torsions (Han et al., 1993). This strongly argues that a negative protein charge, presumably the Glu113 carboxylate side chain, is close to C_{12}.

Bathorhodopsin was modeled starting from the rhodopsin structure described above. The only changes incorporated into the model have been isomerization about the C_{11}═C_{12} bond and the addition of C−C single bond torsions along the retinal chain. The position of the Glu113 side chain relative to the retinal was not refined. This approach was based on several assumptions outlined below.

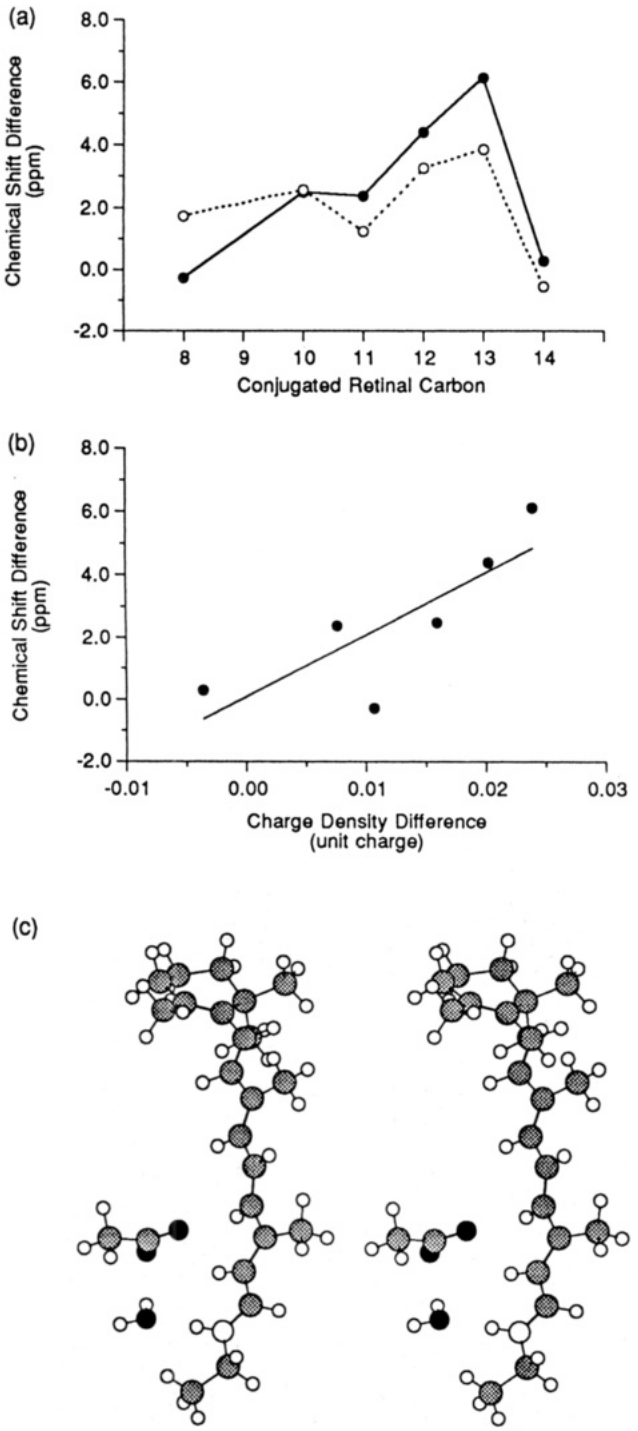

FIGURE 3: Modeling the retinal binding site of bathorhodopsin. (a) Comparison of experimental (●) and calculated (○) chemical shift differences for rhodopsin and the model shown in (c). *all-trans*-RPSB·Cl is used as the reference state. (b) Linear correlation of the chemical shift data with the calculated charge densities of the model. The correlation coefficient is 0.81, the slope is 199 ppm/unit charge and the intercept is 0.06 ppm. (c) Retinal binding site model with a CH_3-COO^- counterion and H_2O hydrogen bonded at the Schiff base. Black symbols stand for O, gray for C, white for N, and small white symbols for H. The key distances are O_1···C_{12} (CH_3-COO^-) 3.0 Å, O_1···H_{12} 2.1 Å, O_1···C_{11} 3.7 Å, O_1···C_{13} 3.8 Å, O_1···N 5.0 Å, O_2···C_{12} (CH_3-COO^-) 5.1 Å, and N···O (water) 2.9 Å.

(1) The position of the Glu113 side chain does not change relative to other protein groups between rhodopsin and bathorhodopsin. The relative position of Glu113 with respect to the retinal, however, does change due to structural changes *in the retinal* from isomerization. Large changes in protein conformation are not expected to occur on the 40 ps time scale of bathorhodopsin formation, although protein deformations due to isomerization may exist (Warshel & Barboy, 1982).

(2) The retinal chromophore in bathorhodopsin is in a twisted *all-trans* conformation. Isomerization about the $C_{11}=C_{12}$ double bond is realized by moving the $C_{12}-H$ and $C_{11}-H$ bonds by 90° in opposite directions. The distance between O_1 and C_{12} is kept at 3.0 Å. This results in a change of the O_1···C_{12}···H_{12} angle θ from 60° in rhodopsin to −30° in bathorhodopsin and a large displacement of the retinal molecule on both sides of the $C_{11}=C_{12}$ double bond. The net displacement is reduced by introducing twists along the C_8-C_9, $C_{10}-C_{11}$, $C_{12}-C_{13}$, and $C_{14}-C_{15}$ single bonds. Evidence for C−C twists of 10−30° about these bonds comes from the intense HOOP modes observed in the bathorhodopsin resonance Raman spectrum (Erying et al., 1980, 1982; Palings et al., 1989). The directions of the C−C twists are chosen to reduce the displacement of the retinal due to isomerization. This constraint argues that the C_8-C_9 and $C_{10}-C_{11}$ twists are in the opposite direction from the $C_{12}-C_{13}$ and $C_{14}-C_{15}$ twists. It is important to recall that the $C_{12}-C_{13}$ bond in rhodopsin is already twisted ~40° from a planar *cis* geometry. We have incorporated a twist of 30° in this torsion angle from the planar *trans* geometry in bathorhodopsin to effectively minimize the displacement of the retinal from C_{13} to the Schiff base upon isomerization. Twists of 20° were incorporated about the other C−C bonds.

(3) The optimal hydrogen bond between the structural water and the Schiff base proton is retained in bathorhodopsin. This is based on the observation that the hydrogen-bonding interactions at the Schiff base are roughly the same in rhodopsin and bathorhodopsin as indicated by the similar C=N stretching frequencies (1657 and 1655 cm^{-1}, respectively) and ND shifts (33 and 26 cm^{-1}, respectively) (Palings et al., 1987). We have changed the position of the water accordingly to maintain a linear hydrogen bond with the Schiff base proton after isomerization.

The model proposed for bathorhodopsin based on the considerations above is presented in Figure 3c, where the retinal chromophore is 11-*trans* with the following torsion angles: $C_7-C_8-C_9-C_{10}$ (−160°), $C_9-C_{10}-C_{11}-C_{12}$ (−160°), $C_{11}-C_{12}-C_{13}-C_{14}$ (150°), and $C_{13}-C_{14}-C_{15}-N$ (160°). The calculated and experimental chemical shift differences are compared in Figure 3a and the quantitative evaluation of the linear correlation is shown in Figure 3b. Since the position of Glu113 was not changed, isomerization changes the angle θ from 60° in rhodopsin to −30° in bathorhodopsin. The 3.0 Å distance between C_{12} and O_1 remains unchanged. The new geometry brings the counterion into a more in-plane orientation with respect to the retinal. The anomalously large upfield shift at C_{12} is reproduced in the calculated chemical shift differences, and the overall fit to the experimental data is good ($R = 0.81$) considering that the positions of the protein charges and retinal structure were not refined. The binding site model also roughly reproduces the red-shift in the absorption maximum (543 nm experimental, 534 nm calculated). The calculated red-shift in the λ_{max} between rhodopsin and bathorhodopsin, from 502 to 534 nm (Table 1), results from the C−C single bond twists in the retinal chain and the more in-plane orientation of the Glu113 carboxylate. Both effects lead to red-shifts in our λ_{max} calculations (data not shown).

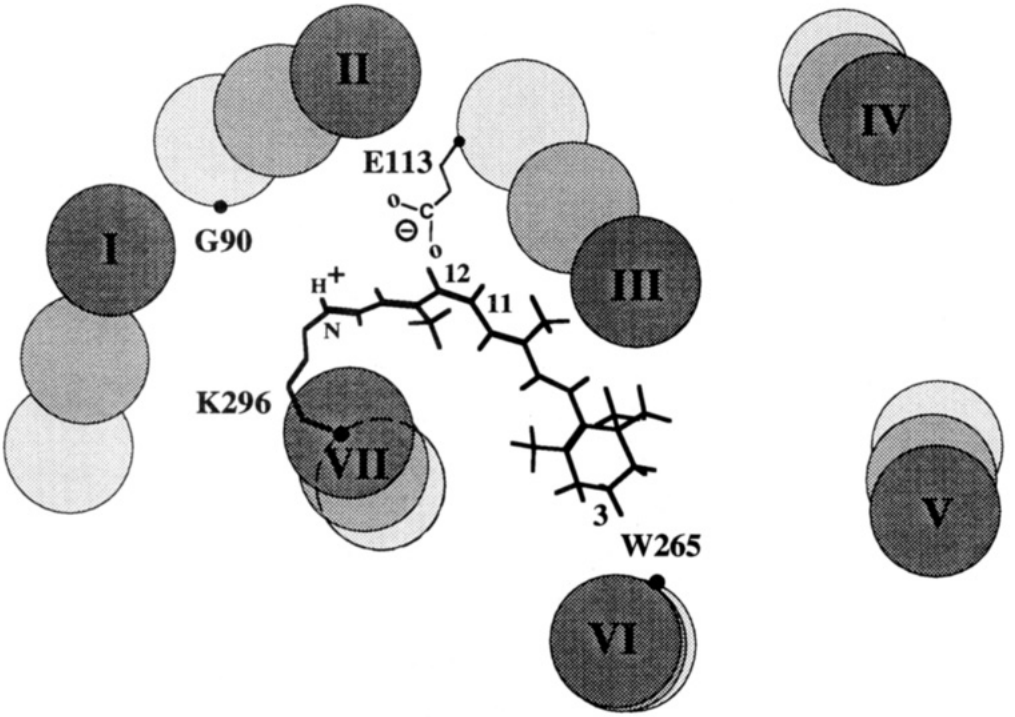

FIGURE 4: Structural model of rhodopsin based on the helix arrangement of Baldwin (1993) and the NMR constraints. The seven transmembrane helices are shown at three levels indicated by differences in shading. The α-carbons of residues of interest are shown in dots of various sizes, indicating the depth from the cytoplasmic domain. Gly90, Glu113, and Lys296, are on the extracellular half of the transmembrane domain and close to each other in space. The 11-*cis*-retinal chromophore has been incorporated into the model using the NMR constraints which require a close interaction between Glu113 and C_{12} of the chromophore. The relative position of the β-ionone ring and Trp265 agree well with recent cross-linking data (Zhang et al., 1994).

The binding site model also provides an explanation for the observation of the uncoupled C_{11}−H and C_{12}−H HOOP modes in bathorhodopsin, but not rhodopsin, even though in both cases the anomalous C_{12} chemical shift is attributed to close interaction of a protein charge. One key difference in the two binding site models is the orientation of the charge relative to the retinal plane. The choice of the 60° orientation for rhodopsin was made in order to produce a more in-plane orientation for bathorhodopsin ($\theta = -30°$), which brings the C_{12} hydrogen closer to O_1 (2.6 vs 2.1 Å) and results in an increased electrostatic interaction. The 2.1 Å H_{12}⋯O_1 distance in bathorhodopsin is shorter than the sum of the van der Waals radii of H and O (1.2 and 1.4 Å, respectively) and is a typical O⋯H distance in a hydrogen bond. This change would potentially lower the frequency of the C_{12}−H HOOP mode and uncouple the out-of-plane motions of C_{11}−H and C_{12}−H hydrogens.

One remaining question concerning the binding site structure of bathorhodopsin involves the mechanism for energy storage. The electrostatic interaction between the retinal PSB and the carboxylate group is very similar for rhodopsin and bathorhodopsin based on the partial charges on each retinal atom and their distance to the two oxygen atoms of the carboxylate counterion. This is in agreement with our earlier estimate of <3 kcal/mol for the energy storage due to charge separation (Smith et al., 1991). The majority of the remaining ~30 kcal/mol of energy must be stored in conformational distortions of the retinal and/or protein and van der Waals repulsions between them. It is important to point out that in both rhodopsin and bathorhodpsin, although O_1 is closest to C_{12}, the strongest electrostatic interactions are between O_1 and the retinal atoms C_{13}, C_{15} and the Schiff base proton due to their much larger partial positive charge. The binding site model suggests that there is a large displacement in the chromophore from C_{11} to the β-ionone ring and a smaller displacement from C_{13} to the Schiff base upon bathorhodopsin formation. It has been shown that the 11-*cis*-retinal binding site in rhodopsin does not accommodate the *all-trans* isomer (Liu & Mirzadegan, 1988). This suggests that the displacement predicted by the bathorhodopsin model results in strong steric interactions and strain in the retinal. Studies on rhodopsin regenerated with retinal analogs provide support for this idea. Retinal analogs have been designed that reduce the rigidity of the retinal or remove steric contacts by (1) saturating the C_5═C_6 or C_7═C_8 double bonds, (2) substituting the ring by acyclic chains, or (3) removing the 13-methyl group (Randall et al., 1991; Jäger et al., 1994a). Rhodopsins regenerated with these retinal analogs all have a common feature, namely, that they form a blue-shifted intermediate rather than bathorhodopsin upon exposure to light. The blue-shifted intermediate exhibits markedly reduced distortion in the retinal as revealed by the lack of intense HOOP modes and a blue-shifted λ_{max} (477 nm). Moreover, most of the artificial rhodopsins listed above result in decreased G-protein activity (Jäger et al., 1994a), suggesting that the rigidity of the retinal molecule and the strong steric contacts in bathorhodopsin are required for efficient G-protein activation.

Location of the Retinal Chromophore in Rhodopsin. Recently, Henderson and co-workers have obtained a 9 Å projection map of rhodopsin (Schertler et al., 1993). In parallel with these studies, Baldwin (1993) has modeled the location, rotational orientation, and tilt of the seven transmembrane helices based on sequence analysis of 204 G-protein-coupled receptors, including rhodopsin. Figure 4 presents a schematic of the Baldwin model where the helices are represented by shaded circles and the position of the α carbons of several residues relevant to the following discus-

sion are indicated. The darkest shading is toward the cytoplasmic surface of the protein. The relative positions and the tilt angles of the helices in this model agrees well with the projection map. Support for this helix arrangement comes from the mutagenesis studies on Gly90 by Oprian and co-workers. They have found that in the mutants G90D and G90D/E113A, Asp90 can either compete with or replace Glu113 as the Schiff base counterion (Rao et al., 1994). This implies close proximity of residue 90 to the Schiff base, as predicted by the model.

We are able to position the retinal in the interior of the protein using the constraints derived from the NMR and absorption data. As shown in Figure 4, the proposed Glu113⁻retinal C_{12} interaction depicted in Figure 2d can be readily accommodated in the Baldwin model given the shape of the protein interior and the rotational orientations of helices III and VII, on which the two key amino acids, Glu113 and Lys296, reside. Glu113 is located near the intradiscal end of helix III and approaches C_{12} from beneath the retinal plane. Fluorescence energy transfer (Thomas & Stryer, 1982) and linear dichroism (Liebman, 1962) measurements indicate that the retinal is located in the center of the lipid bilayer with its transition dipole oriented at an angle of ~16° with respect to the membrane plane. It is necessary to place the retinal plane roughly perpendicular to the helix axis in order to account for these observations and to reproduce the geometry shown in Figure 2d.

There are several additional observations that can be explained by the proposed location of the retinal. First, the λ_{max} of the retinal chromophore is sensitive to the relative distance between the Schiff base and the carboxylate counterion; the λ_{max} shifts to the red with longer separations. This can explain the 5−10 nm red-shift observed in the E113D mutant, where the shorter aspartic acid side chain would be expected to increase the distance to the Schiff base (Sakmar et al., 1989, 1991; Zhukovsky & Oprian, 1989). The model in Figure 4 predicts that the Schiff base is closer to residue 90 than to 113. This is consistent with the fact that in G90D/E113Q mutant, where Asp90 is the counterion, the λ_{max} [472 nm (Rao et al., 1994)] is blue-shifted compared to that of rhodopsin (500 nm) or the E113D mutant (~510 nm). Second, the β-ionone ring is positioned between helices III and VI in Figure 4. Recent cross-linking experiments by Nakanishi and co-workers have shown that a photoactivatable group at position C_3 of the β-ionone ring reacts specifically with two adjacent residues on helix VI, Trp265 and Leu266 (Zhang et al., 1994). This result is in excellent agreement with the model, where C_3 is predicted to be in close proximity to Trp265 (Figure 4). The retinal analog used for this study has an 11-*cis* configuration locked by a six-membered ring and consequently cannot isomerize during the photoactivated cross-linking reaction. This is in contrast with the previous experiments of Khorana and co-workers where a number of cross-linking sites, including Trp265, were found on both helices III and VI (Nakayama & Khorana, 1990). The cross-linking at multiple sites may be due to a change of orientation of the β-ionone ring during the *cis*−*trans* photoisomerization of the retinal caused by photoexcitation of the cross-linking group. This is in agreement with the structural changes occurring in the formation of bathorhodopsin, where we would predict that C_3 is reoriented toward helix III when the retinal conformation in bathorhodopsin shown in Figure 3c is incorporated into the apoprotein in Figure 4. Further evidence for the crucial role of Trp265 in the retinal binding site is provided by mutagenesis studies. Substitutions of Trp265 by Tyr, Phe, or Ala result in a marked reduction in retinal regenerability and G-protein activation upon exposure to light (Nakayama & Khorana, 1991). The detrimental effects of mutations at this position are more pronounced with the decreased size of the substituent, implying that Trp265 forms one boundary of the retinal binding site.

It is important to realize that the retinal molecule in rhodopsin is actually chiral due to twists about the C_6-C_7 and $C_{12}-C_{13}$ single bonds (see Materials and Methods). The mirror image of the structure shown in Figure 2d yields the same calculated charge densities and λ_{max} and therefore fits the experimental data equally well. However, only the geometry shown in Figure 2d, but not its enantiomer, can be incorporated into the chiral binding site defined by the seven helices. This constraint allows us to assign the $C_{11}-C_{12}-C_{13}-C_{14}$ torsion angle as +140° rather than −140°. The absolute torsion angle of the $C_5-C_6-C_7-C_8$, on the other hand, has not yet been established.

In summary, these studies extend our previous results (Han et al., 1993) by refining the location of the counterion relative to the retinal in rhodopsin. The orientations of both negatively charged oxygens of the carboxylate are established, where one oxygen is closest to C_{12} and the other is oriented away from the retinal chain. These constraints can be used to position the 11-*cis*-retinal chromophore in the interior of the rhodopsin apoprotein (Baldwin, 1993). This model can serve as a starting point for suggesting how retinal isomerization leads to protein activation through each intermediate of the photoreaction. In this paper, we discussed the structure of the first intermediate, bathorhodopsin. The retinal binding site for rhodopsin is able to accommodate 11-*cis*, but not 11-*trans*, retinal. Rapid photoisomerization of the retinal generates a conformationally distorted 11-*trans* chromophore that has large steric contacts with the protein, responsible for most, if not all, of the 33 kcal/mol of energy stored in this intermediate. The retinal binding site model of bathorhodopsin can be generated based on rhodopsin and several simple assumptions (Figure 3c). It fits both the chemical shift and the absorption data moderately well without further refinement. It also provides an explanation for the the red-shift in bathorhodopsin λ_{max} and the puzzling observation of the uncoupled $C_{11}-H$ and $C_{12}-H$ HOOP modes. After bathorhodopsin, the distortion seems to be transferred from the retinal to the protein moiety of the pigment, since in the subsequent photointermediates, the retinal appears undistorted (Jäger et al., 1994a). Relaxation of the protein leads to a change in the Glu-113⁻Schiff base interaction in these intermediates and eventually results in Schiff base deprotonation and the simultaneous protonation of Glu113 (Fahmy et al., 1994; Jäger et al., 1994b) in metarhodopsin II. Protein conformational changes that occur in the formation of metarhodopsin II lead to G-protein activation.

ACKNOWLEDGMENT

We thank Dr. Joyce Baldwin for providing diagrams for the arrangement of the seven helices and Prof. Johan Lugtenburg for catalyzing the ^{13}C NMR measurements on rhodopsin.

REFERENCES

Albeck, A., Livnah, N., Gottlieb, H., & Sheves, M. (1992) *J. Am. Chem. Soc. 114*, 2400−2411.

Bagley, K. A., Balogh-Nair, V., Croteau, A. A., Dollinger, G., Ebrey, T. G., Eisenstein, L., Hong, M. K., Nakanishi, K., & Vittitow, J. (1985) *Biochemistry 24*, 6055−6071.
Baldwin, J. M. (1993) *EMBO J. 12*, 1693−1703.
Bassov, T., Friedman, N., & Sheves, M. (1987) *Biochemistry 26*, 3210−3217.
Birge, R. R. (1993) *Biophys. J. 64*, 1371−1372.
Birge, R. R., Murray, L. P., Pierce, B. M., Akita, H., Balogh-Nair, V., Findsen, L. A., & Nakanishi, K. (1985) *Proc. Natl. Acad. Sci. U.S.A. 82*, 4117−4121.
Birge, R. R., Einterz, C. M., Knapp, H. M., & Murray, L. P. (1988) *Biophys. J. 53*, 367−385.
Blatz, P. E., Mohler, J. H., & Navangul, H. V. (1972) *Biochemistry 11*, 848−855.
Cohen, G. B., Oprian, D. D., & Robinson, P. R. (1992) *Biochemistry 31*, 12592−12601.
Cooper, A. (1979) *Nature 282*, 531−533.
Cossette, D., & Vocelle, D. (1987) *Can. J. Chem. 65*, 1576−1583.
Deng, H., Huang, L., Callender, R., & Ebrey, T. (1994) *Biophys. J. 66*, 1129−1136.
Eyring, G., Curry, B., Mathies, R., Fransen, R., Palings, I., & Lugtenburg, J. (1980) *Biochemistry 19*, 2410−2418.
Eyring, G., Curry, B., Broek, A., Lugtenburg, J., & Mathies, R. (1982) *Biochemistry 21*, 384−393.
Fahmy, K., Jäger, F., Beck, M., Zvyaga, T. A., Sakmar, T. P., & Siebert, F. (1993) *Proc. Natl. Acad. Sci. U.S.A. 90*, 10206−10210.
Gat, Y., & Sheves, M. (1993) *J. Am. Chem. Soc. 115*, 3772−3773.
Gilardi, R. D., Karle, I. L., & Karle, J. (1972) *Acta Crystallogr. B28*, 2605−2612.
Han, M., DeDecker, B. S., & Smith, S. O. (1993) *Biophys. J. 65*, 899−906.
Honig, B., & Karplus, M. (1971) *Nature 229*, 558−560.
Honig, B., Greenberg, A. D., Dinur, U., & Ebrey, T. G. (1976) *Biochemistry 15*, 4593−4599.
Honig, B., Dinur, U., Nakanishi, K., Balogh-Nair, V., Gawinowicz, M. A., Arnaboldi, M., & Motto, M. G. (1979) *J. Am. Chem. Soc. 101*, 7084−7086.
Jäger, F., Jäger, S., Kräutle, O., Friedman, N., Sheves, M., Hofmann, K. P., & Siebert, F. (1994a) *Biochemistry 33*, 7389−7397.
Jäger, F., Fahmy, K., Sakmar, T. P., & Siebert, F. (1994b) *Biochemistry 33*, 10878−10882.
Koutalos, Y., Ebrey, T. G., Tsuda, M., Odashima, K., Lien, T., Park, M. H., Shimizu, N., Derguini, F., Nakanishi, K., Gilson, H. R., & Honig, B. (1989) *Biochemistry 28*, 2732−2739.
Kropf, A., & Hubbard, R. (1958) *Ann. N.Y. Acad. Sci. 74*, 266−280.
Kühn, H. (1980) *Nature 283*, 587−589.
Lauterbur, P. C. (1961) *J. Am. Chem. Soc. 83*, 1838−1846.
Liebman, P. A. (1962) *Biophys. J. 2*, 161−178.
Liu, R. S. H., & Mirzadegan, T. (1988) *J. Am. Chem. Soc. 110*, 8617−8623.
Mathies, R., Freedman, T. B., & Styer, L. (1977) *J. Mol. Biol. 109*, 367−372.
Nakayama, T. A., & Khorana, H. G. (1990) *J. Biol. Chem. 265*, 15762−15769.
Nakayama, T. A., & Khorana, H. G. (1991) *J. Biol. Chem. 266*, 4269−4275.
Narva, D., & Callender, R. H. (1980) *Photochem. Photobiol. 32*, 273−276.
Nathans, J. (1990) *Biochemistry 29*, 9746−9752.
Oprian, D. D. (1992) *J. Bioenerg. Biomembr. 24*, 211−217.
Palings, I., Pardoen, J. A., van den Berg, E. M. M., Winkel, C., Lugtenburg, J., & Mathies, R. A. (1987) *Biochemistry 26*, 2544−2556.
Palings, I., van den Berg, E. M. M., Lugtenburg, J., & Mathies, R. A. (1989) *Biochemistry 28*, 1498−1507.
Rafferty, C. N., & Shichi, H. (1981) *Photochem. Photobiol. 33*, 229−234.
Randall, C. E., Lewis, J. W., Hug, S. J., Bjorling, S. C., Eisner-Shanas, I., Friedman, N., Ottolenghi, M., Sheves, M., & Kliger, D. S. (1991) *J. Am. Chem. Soc. 113*, 3473−3485.
Rao, V. R., Cohen, G. B., & Oprian, D. D. (1994) *Nature 367*, 639−642.
Resek, J. F., Farahbakhsh, Z. T., Hubbell, W. L., & Khorana, H. G. (1993) *Biochemistry 32*, 12025−12032.
Robinson, P. R., Cohen, G. B., Zhukovsky, E. A., & Oprian, D. D. (1992) *Neuron 9*, 719−725.
Rodman-Gilson, H. S., & Honig, B. (1988) *J. Am. Chem. Soc. 110*, 1943−1950.
Rodman-Gilson, H. S., Honig, B. H., Croteau, A., Zarrilli, G., & Nakanishi, K. (1988) *Biophys. J. 53*, 261−269.
Rothschild, K. J., Gillespie, J., & DeGrip, W. (1987) *Biophys. J. 51*, 345−350.
Sakmar, T. P., Franke, R. R., & Khorana, H. G. (1989) *Proc. Natl. Acad. Sci. U.S.A. 86*, 8309−8313.
Sakmar, T. P., Franke, R. R., & Khorana, H. G. (1991) *Proc. Natl. Acad. Sci. U.S.A. 88*, 3079−3083.
Scheiner, S., & Hillenbrand, E. A. (1985) *Proc. Natl. Acad. Sci. U.S.A. 82*, 2741−2745.
Scheiner, S., & Duan, X. (1991) *Biophys. J. 60*, 874−883.
Schertler, G. F., Villa, C., & Henderson, R. (1993) *Nature 362*, 770−772.
Schick, G. A., Cooper, T. M., Holloway, R. A., Murray, L. P., & Birge R. R. (1987) *Biochemistry 26*, 2556−2562.
Schoenlein, R. W., Peteanu, L. A., Mathies, R. A., & Shank, C. V. (1991) *Science 254*, 412−415.
Shriver, J. W., Abrahamson, E. W., & Mateescu, G. D. (1976) *J. Am. Chem. Soc. 98*, 2407−2409.
Shriver, J. W., Mateescu, G. D., & Abrahamson, E. W. (1979) *Biochemistry 18*, 4785−4792.
Smith, S. O., Palings, I., Miley, M. E., Courtin, J., de Groot, H., Lugtenburg, J., Mathies, R. A., & Griffin, R. G. (1990) *Biochemistry 29*, 8158−8164.
Smith, S. O., Courtin, J., de Groot, H., Gebhard, R., & Lugtenburg, J. (1991) *Biochemistry 30*, 7409−7415.
Spiesecke, H., & Schneider, W. G. (1961) *Tetrahedron Lett. 14*, 468−472.
Steinberg, G., Ottolenghi, M., & Sheves, M. (1993) *Biophys. J. 64*, 1499−1502.
Strader, C. D., Fong, T. M., Tota, M. R., & Underwood, D. (1994) *Annu. Rev. Biochem. 63*, 101−132.
Tallent, J. R., Hyde, E. W., Findsen, L. A., Fox, G. C., & Birge, R. R. (1992) *J. Am. Chem. Soc. 114*, 1581−1592.
Thomas, D. D., & Stryer, L. (1982) *J. Mol. Biol. 154*, 145−157.
Tokuhiro, T., & Fraenkel, G. (1969) *J. Am. Chem. Soc. 91*, 5005−5013.
Warshel, A., & Barboy, N. (1982) *J. Am. Chem. Soc. 104*, 1469−1476.
Zhukovsky, E. A., & Oprian, D. D. (1989) *Science 246*, 928−930.
Zhang, H., Lerro, K. A., Yamamoto, T., Lien, T. H., Sastry, L., Gawinowicz, M. A., & Nakanishi, K. (1994) *J. Am. Chem. Soc.* (in press).
Zvyaga, T. A., Fahmy, K., & Sakmar, T. P. (1994) *Biochemistry 33*, 9753−9761.

BI942295X